Interfacial Polymerization on Dynamic Complex Colloids: Creating Stabilized Janus Droplets

Citation: He, Yuan et al."Interfacial Polymerization on Dynamic Complex Colloids: Creating Stabilized Janus Droplets." ACS Applied Materials & Interfaces 9, 8 (February 2017): 7804–7811

As Published: http://dx.doi.org/10.1021/acsami.6b15791

Publisher: American Chemical Society (ACS)

Persistent URL: http://hdl.handle.net/1721.1/115099

Version: Author's final manuscript: final author's manuscript post peer review, without publisher's formatting or copy editing

Interfacial Polymerization on Dynamic Complex Colloids: Creating Stabilized Janus Droplets

Yuan He[a], Suchol Savagatrup[a], Lauren D. Zarzar[a,b] and Timothy M. Swager[a]*

[a] *Department of Chemistry and Institute for Soldier Nanotechnologies, Massachusetts Institute of Technology, Cambridge MA 02139, United States*

[b] *Department of Materials Science and Engineering and Department of Chemistry, Pennsylvania State University, State College, PA 16801, United States*

Interfacial polymerization, dynamic complex colloids, Janus droplets

ABSTRACT: Complex emulsions, including Janus droplets, are becoming increasingly important in pharmaceuticals and medical diagnostics, the fabrication of microcapsules for drug delivery, chemical sensing, E-paper display technologies, and optics. Because fluid Janus droplets are often sensitive to external perturbation, such as unexpected changes in the concentration of the surfactants or surface-active biomolecules in the environment, stabilizing their morphology is critical for many real-world applications. To endow Janus droplets with resistance to external chemical perturbations, we demonstrate a general and robust method of creating polymeric hemispherical shells via interfacial free-radical polymerization on the Janus droplets. The polymeric hemispherical shells were characterized by optical and fluorescence microscopy, scanning electron microscopy (SEM), and confocal laser scanning microscopy (CLSM). By comparing phase diagrams of a regular Janus droplet and a Janus droplet with the hemispherical shell, we show that the formation of the hemispherical shell nearly doubles the range of the Janus morphology and maintains the Janus morphology upon certain degree of external perturbation (e.g. adding hydrocarbon-water or fluorocarbon-water surfactants). We attribute the increased stability of the Janus droplets to (1) the surfactant nature of polymeric shell formed and (2) increase in interfacial tension between hydrocarbon and fluorocarbon due to polymer shell formation. This finding opens the door of utilizing these stabilized Janus droplets in demanding environment.

Introduction

One of the most important motivations for research in the field of complex emulsions is the promise of real-world applications in pharmaceuticals and medical diagnostics,[1,2] microcapsule fabrication for drug delivery,[3–6] chemical sensing,[7] and food industry.[8,9] Janus droplets are a special member of complex emulsions with different chemistries, polarities, or

functionalities on each side and have also found wide range of applications including optical probes for chemical and biological measurements,[10,11] artificial ink for E-paper display technologies,[12,13] and *in vivo* delivery of biomedicine.[14] The defining advantages of Janus droplets derive from their multi-functionality, anisotropic property, and structural complexity compared to conventional homogeneous micro/nano emulsions.[15,16] However, challenges remain in the preservation of Janus morphology. Newly-formed Janus droplets are thermodynamically unstable in certain conditions and transform either into a core-shell structure when one phase strongly disfavors the outside medium or merge into a single-phase structure when one phase is soluble in the other.[17–19] One solution to the fragility of this structure is to polymerize one or both phases of the Janus droplets and "freeze" the Janus morphology after their formation and before any phase transformation can occur.[20] Although this strategy offers increased stability, polymerization essentially changes the nature of fluid Janus droplets, especially their optical properties, which can limit applications in certain areas such as dynamic optics.[21] There remains a need to stabilize fluid Janus droplets without altering their optical properties.

We envisioned that the Janus droplets could be stabilized by forming a hemispherical shell consisting of a layer of crosslinked polymer at the aqueous interface of one of the phases. This hemispherical shell may mechanically prohibit the transformation from Janus droplets to double emulsions. Furthermore, using interfacial polymerization, thin polymeric hemispherical shells can be formed, preserving the original optical properties of fluid Janus droplets.

Our dynamic complex emulsions are made of hydrocarbon (H) and fluorocarbon (F) in water (W).[22] They are capable of switching reversibly between two double emulsion morphologies (abbreviated as H/F/W and F/H/W thereafter) and the Janus morphology depending on the concentration and effectiveness of the external surfactants (**Figure 1a**).[22] The unique optical properties of the Janus morphology can be exploited in a variety of chemical and biochemical sensing applications.[23,24] Thus, stabilizing the Janus morphology to external perturbation is crucial to their applications in complex environments. Herein, we report the stabilization of the Janus morphology of dynamic complex emulsions by creating a polymeric hemispherical shell on the hydrocarbon hemisphere of the Janus droplets. Janus droplets with the polymer shells showed resistance to switching of morphology upon external perturbation (*i.e.* adding excess hydrocarbon-water or fluorocarbon-water surfactants), leading to the increased range of the Janus morphology of nearly 100%.

Results and discussion

Synthesis of the polymeric hemispherical shells

The Janus droplets used in this study consisted of hexadecane with 20 wt% dibutyl maleate as hydrocarbon phase (H) and ethyl nonafluorobutylether as fluorocarbon phase (F). Polydisperse Janus droplets were fabricated through bulk emulsification of equal volume mixture of H and F, which were pre-heated above their upper critical solution temperature. We first made hemispherical shells via interfacial free-radical polymerization on the hydrocarbon-water interface of the Janus droplets. Dibutyl maleate dissolved in hexadecane served as the oil-phase monomer and PEG-divinylether served as the water-phase monomer.

It had been previously demonstrated that this combination will give selective interfacial polymerization when a co-localized cationic interfacial initiator was used (**4** in **Figure 1b**).[25] The interfacial initiator **4** is a surfactant, but was inadequate in stabilizing the dynamic complex fluid emulsions. As a result, Triton X-100 was added as a hydrocarbon-water co-surfactant (interfacial initiator:Triton X-100 = 1:2 by mass, referred to as "hydrocarbon-water surfactant" hereafter) and the fluorocarbon-water interface was stabilized by a single fluorocarbon surfactant (Zonyl FS-300, hereafter "Zonyl"). In order to directly visualize the formation of hemispherical shells on the Janus droplets, we synthesized and incorporated an emissive water-phase co-monomer, naphthalene diimide (NDI) labeled monovinylether **3** (**Figure 1c**).

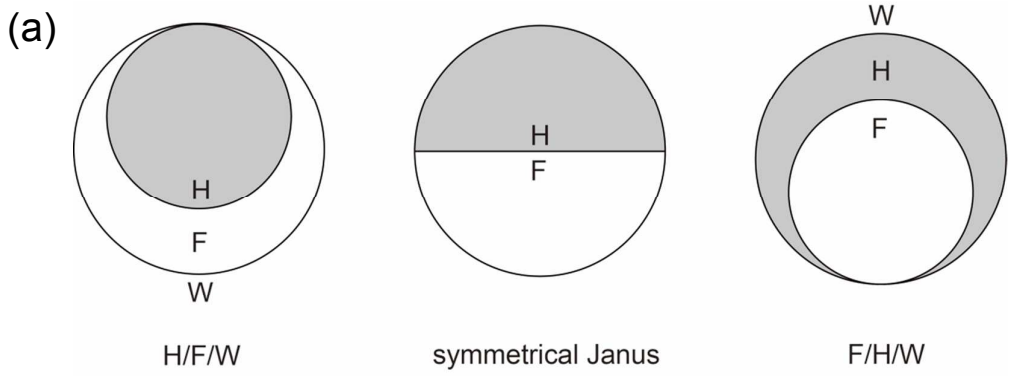

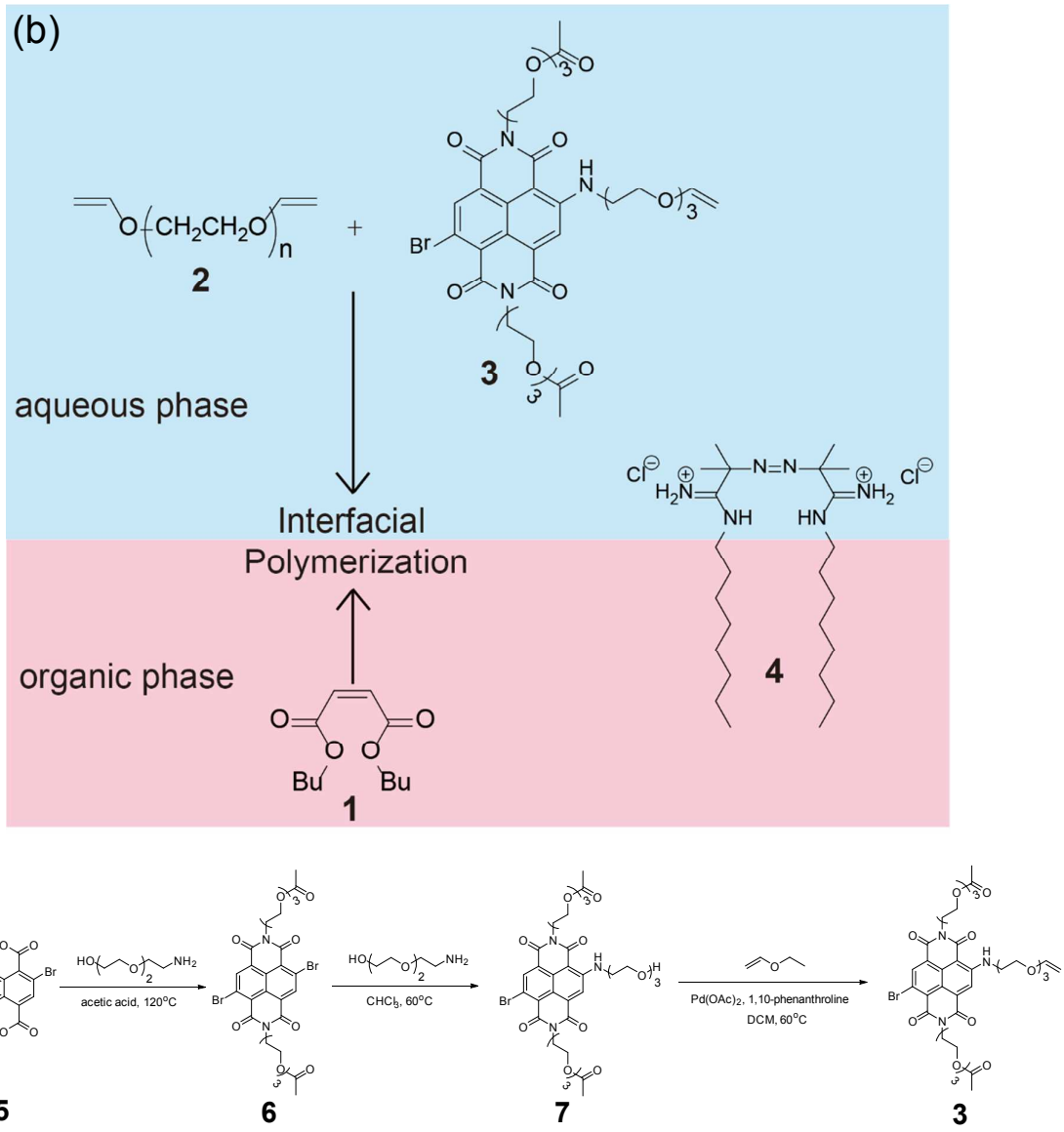

Figure 1. (a) Schematic representation of three different morphologies of dynamic complex emulsions (b) Interfacial free-radical polymerization of dibutyl maleate **1** with PEG-divinylether **2** and NDI-monovinylether **3**, initiated by surface-active initiator **4** at hydrocarbon-water interface under 365nm UV (c) Synthesis of NDI-monovinylether **3**.

NDI was selected as fluorophore due to its photostability as well as its chemical inertness to extended UV irradiation and attack by free-radicals.[26] NDI-monovinylether **3** displayed a yellow-greenish fluorescence upon 473 nm excitation. In all following studies, a mixture of PEG-divinylether and NDI-monovinylether **3** (4:1 by mass) was used for interfacial polymerization. Here NDI-monovinylether **3** with only one polymerization site served as the

minor component of water-phase monomers; it was not expected to compromise the crosslinked nature of the polymeric shells. To suppress oxygen quenching upon free-radical polymerization, the solution containing Janus droplets was sparged with nitrogen for 10 min before UV exposure.

Characterization of polymeric hemispherical shell

Before imaging, the residual NDI-monovinylether in water was removed by solvent exchange with the same surfactant solution without the water-phase monomers to reduce background fluorescence. Typical bright field, fluorescence, and transient images of the resultant Janus droplets after interfacial polymerization are shown in **Figure 2**. Emulsions were agitated to induce tumbling of the droplets such that the transient images could be captured with an exposure of 1 ms.

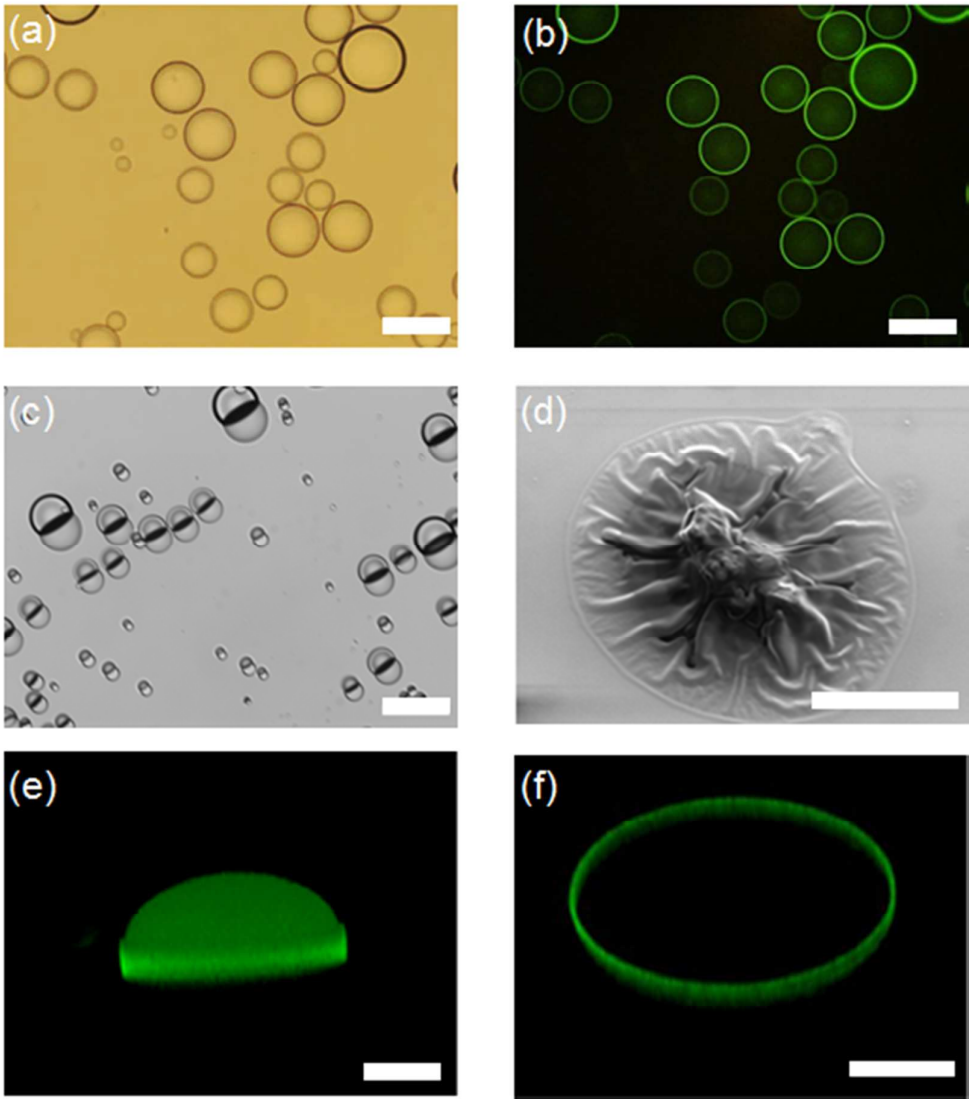

Figure 2. Characterization of Janus droplets with polymeric hemispherical shells (a) Bright field image (b) fluorescence image upon 473 nm excitation and (c) transient image of Janus droplets after interfacial polymerization and removal of excess **3**. (d) SEM image of hemispherical shells after drying in vacuum oven for overnight. (e) 3D visualization of a hemispherical shell. (f) The bottom portion of a hemispherical shell. Scale bars in (a), (b) and (c): 200μm, and scale bars in (d), (e) and (f): 50 μm

The formation of the hemispherical shell was confirmed by the green fluorescence selectively localized at the hydrocarbon-water interface in **Figure 2b**. The fluorescent rings of smaller droplets in **Figure 2b** appeared dimer because they were out of focus. **Figure 2c** reveals that the Janus morphology was maintained after interfacial polymerization and **Figure**

2d shows an image of the solid residual of hemispherical shells after drying in vacuum oven overnight. The hemispherical shells shrank and wrinkled in high vacuum, which was typical of polymeric hollow capsules and vesicles made through other methods.[27] Using a confocal laser scanning microscope (CLSM), we were able to further characterize hemispherical shells in 3D (**Figure 2e** and **2f**). Because gravity oriented the Janus droplets with denser fluorous phase downward, we proved that the interfacial polymerization only occurred at the hydrocarbon-water interface because only the top hemisphere in **Figure 2e** emitted green fluorescence. **Figure 2f** shows the bottom portion of a hemispherical shell and confirms that the polymer was only present at the interface. Most importantly, we found that the formation of hemispherical shells on the Janus droplets had negligible effect on their optical transparency in z-direction after *in-situ* UV polymerization (**Figure S3**). This result could be explained by the small thickness of polymer shells formed, which was estimated previously to be on the order of ~10 nm by transmission electron microscopy (TEM).[25]

Expansion of the range of the Janus morphology

After confirming the formation of hemispherical shells on Janus droplets, we endeavored to test if the hemispherical shells could inhibit the morphological transformation of Janus droplets into double emulsions (H/F/W or F/H/W, **Figure 1a**). The changes in the morphology of droplets were monitored when surfactant concentrations in solution were systematically perturbed. To gradually drive the system towards F/H/W, we incrementally added aliquots of 0.2 wt% solution of hydrocarbon-water surfactant. Alternatively, to drive the system towards H/F/W, we incrementally added aliquots of 0.2 wt% solution of Zonyl instead. From here forward we will refer to the changes in concentration of surfactants in

solution by volume ratio of surfactant-containing solution. For example, 70% hydrocarbon-water surfactant will indicate that we have changed the solution to contain 70% by volume of the 0.2 wt% hydrocarbon-water surfactant solution (the remaining 30% by volume is 0.2 wt% Zonyl solution). Alternatively, 70% Zonyl will indicate that we have changed the solution to be 70% by volume of 0.2 wt% Zonyl solution (the remaining 30% by volume is 0.2 wt% hydrocarbon-water surfactant solution).

In order to make a comparison, we first constructed a regular phase diagram of dynamic complex emulsions without hemispherical shells, *i.e.*, a diagram that describes droplet morphology at different hydrocarbon-water surfactant volume ratios (**Figure 3**, top row). Hexadecane containing 20 wt% dibutyl maleate served as hydrocarbon phase and ethyl nonafluorobutylether served as fluorocarbon phase. Dynamic complex emulsions were independently emulsified at each listed hydrocarbon-water surfactant volume ratios.

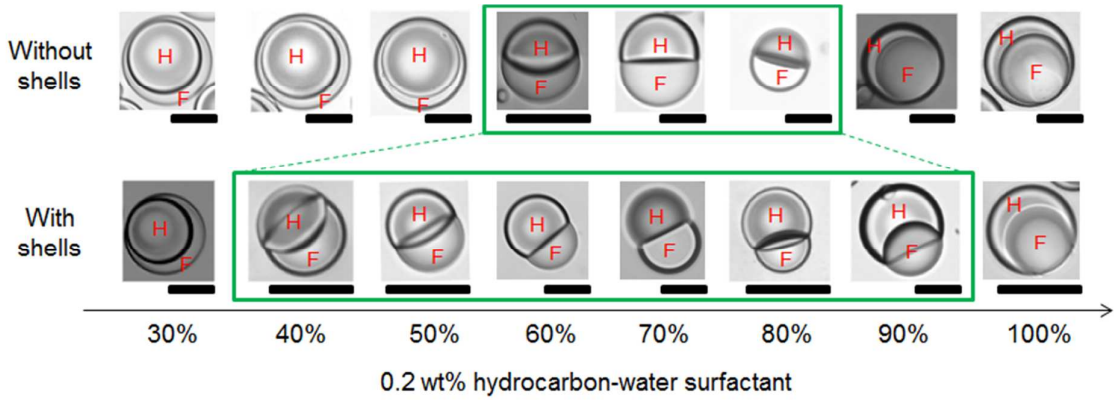

Figure 3. Phase behavior of dynamic complex emulsions without hemispherical shells (top row) and modified phase behavior of dynamic complex emulsions with hemispherical shells (bottom row). The droplets inside the green boxes in (a) and (b) define the range of the Janus morphology. Note: for the bottom row, polymer shells remained intact on the droplets in all cases except 30% hydrocarbon-water surfactant where polymer shells had dissociated from droplets. Scale bars: 50 μm

Here we defined a droplet as having the Janus morphology as long as one of its phases does not completely encapsulate the other phase. According to the top row of **Figure 3**, droplets took H/F/W morphology when the volume ratio of hydrocarbon-water surfactant was below 60% and F/H/W morphology when the volume ratio of hydrocarbon-water surfactant was above 80%. Detailed investigation confirmed the range of Janus morphology to be from 55% to 85% hydrocarbon-water surfactant (**Figure S5**). Here cropped images of droplets were used due to their polydispersity; while all droplets in a full image were uniform in morphology, only a few were in focus. Examples of the full images are shown in **Figure S6**. As demonstrated previously, droplet morphology is controlled by three interfacial tensions: γ_H, γ_F and γ_{HF}.[22] γ_H, γ_F, and γ_{HF} represent the interfacial tension between hydrocarbon-water interface, fluorocarbon-water interface and hydrocarbon-fluorocarbon interface respectively. When γ_{HF} is significantly smaller than the other two, droplets adopt spherical conformation to minimize total hydrocarbon-water and fluorocarbon-water interfacial area. As γ_{HF} increases, droplets tend to minimize hydrocarbon-fluorocarbon interfacial area and become "snowman-shaped."[28] All droplets without hemispherical shells shown in the top row of **Figure 3** appeared spherical in shape, indicating insignificant hydrocarbon-fluorocarbon interfacial tension. We also observed the symmetrical Janus droplets to appear at 70% hydrocarbon-water surfactant.

After constructing the regular phase diagram, interfacial polymerization was performed on symmetrical Janus droplets at 70% hydrocarbon-water surfactant. After confirming the shell formation via fluorescence microscope, droplet morphologies with hemispherical shells at various hydrocarbon-water surfactant volume ratios were obtained by adding either an

excess of 0.2 wt% hydrocarbon-water surfactant solution (for morphologies above 70% hydrocarbon-water surfactant) or an excess of 0.2 wt% Zonyl solution (for morphologies below 70% hydrocarbon-water surfactant) before imaging. Solvent exchange with pure 0.2 wt% hydrocarbon-water surfactant solution gave 100% hydrocarbon-water surfactant. We found that Janus droplets with polymer shells adopted non-spherical or "snowman-shaped" conformation compared to those without shells (**Figure 3**, bottom row), indicating increased interfacial tension between hydrocarbon and fluorocarbon, which may be the result of dibutyl maleate consumption (**Figure S2** for hydrocarbon-fluorocarbon interfacial tension vs. dibutyl maleate wt%). Morphologies of droplets with hemispherical shells at various hydrocarbon-water surfactant volume ratios are summarized in the bottom row of **Figure 3**. Detailed investigation confirmed the Janus morphology at 95% hydrocarbon-water surfactant and H/F/W morphology at 35% hydrocarbon-water surfactant for droplets with polymer shells (**Figure S5**). By tracking the fluorescence from polymeric shells, we found that they dissociated from the droplets at around 35% hydrocarbon-water surfactant because the ring-shaped fluorescence images disappeared and the fluorescence was localized to aggregates of polymer shells (**Figure 4a)**. However, the shells and droplets remained intact at hydrocarbon-water surfactant volume ratios above 70% (**Figure 4b**). The less intense fluorescence brightness in **Figure 4b** was the result of scattering by the F/H/W double emulsions with incident excitation light.

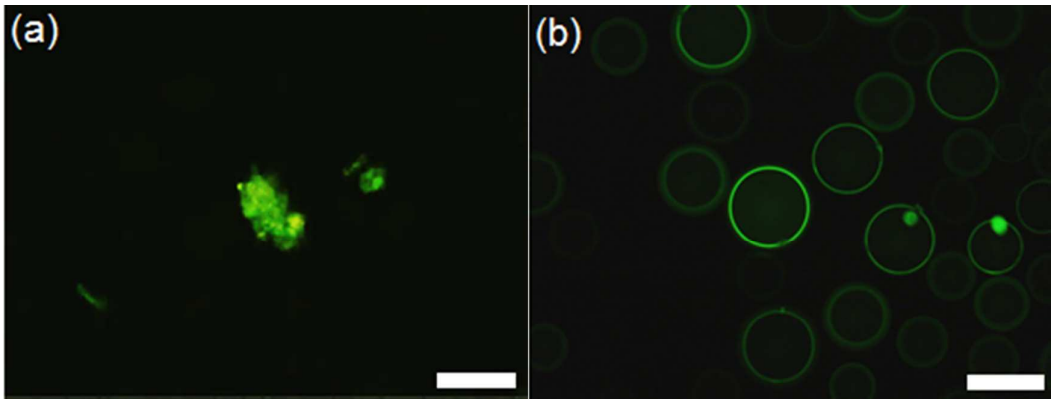

Figure 4. (a) Tracking fluorescence from the polymer shells at 35% hydrocarbon-water surfactant (b) Tracking fluorescence from the polymer shells at 100% hydrocarbon-water surfactant. Scale bars: 200 μm

From the bottom row of **Figure 3**, we found that the range over which the Janus morphology was stable was nearly doubled (from 40% to 95% hydrocarbon-water surfactant) compared to the case without hemispherical shells (from 55% to 85% hydrocarbon-water surfactant). This result indicated that the formation of hemispherical shells created Janus droplets that were resistant to morphological changes upon large surfactant concentration change in solution. To better demonstrate this phenomenon quantitatively, we had endeavored to characterize the "degree of Janus" of a droplet based on its transient image, *i.e.* how close the droplet is to a symmetrical Janus droplet. An example of analysis is illustrated in the inset of **Figure 5** wherein the junction point where all three phases (H, F, and W) came into contact was first determined and then three tangential lines representing the direction of γ_H, γ_F and γ_{HF} were drawn. By definition, the angle between γ_H and γ_{HF} is θ_H and angle between γ_F and γ_{HF} is θ_F. We decided to use θ_F to estimate degree of Janus for all transient images of droplets in **Figure 3** as a result of the fact that θ_F is 90 degrees in the symmetrical Janus state, 0 degree represents a H/F/W double emulsion, and 180 degrees indicates a F/H/W double emulsion. The results of this analysis are summarized in **Figure 5**.

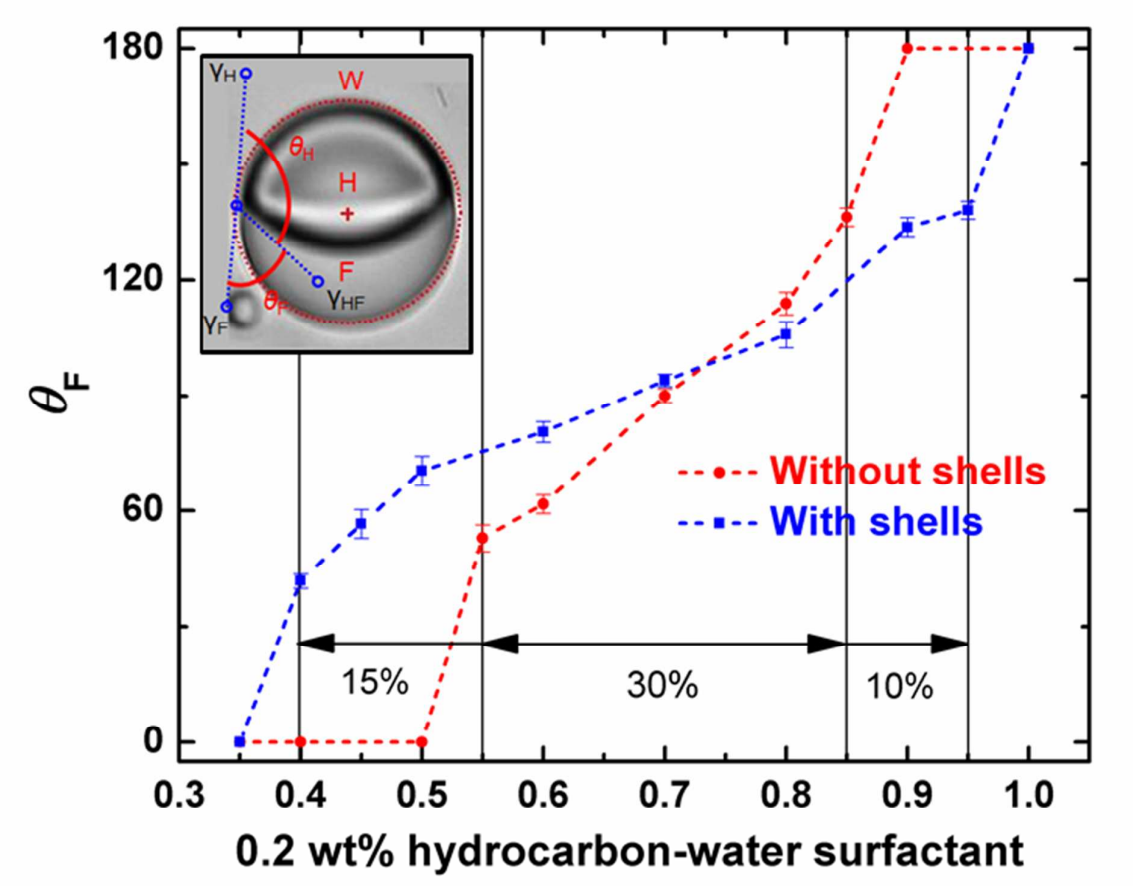

Figure 5. θ_F vs. hydrocarbon-water surfactant volume ratio. Inset: example of "degree of Janus" estimation based on the transient image of Janus droplets without shells at 60% hydrocarbon-water surfactant. Three blue lines represent the direction of three interfacial tensions while their lengths are arbitrary

In **Figure 5**, for droplets without the shells, θ_F increased sharply with respect to hydrocarbon-water surfactant volume ratio from 55% to 85%. However for droplets with the shells, the upward slope of θ_F was reduced significantly from 40% to 95% hydrocarbon-water surfactant, which indicated a stronger tendency to stay in the Janus morphology. As a result, the range of Janus morphology was expanded 15% on the left (towards H/F/W) and 10% on the right (towards F/H/W).

Explanation for the expansion of Janus stability relative to H/F/W and F/H/W

We attributed the increased stability of Janus droplets to (1) the polymer shells which are wrapping the hydrocarbon hemisphere of Janus droplets and (2) hydrocarbon-fluorocarbon interfacial tension increase resulting from polymer shell formation. In the bottom row of **Figure 3**, hexadecane (hydrocarbon phase) contained 20 wt% dibutyl maleate before UV exposure (same as the "without shells" case, **Figure 3** top row) but some dibutyl maleate in hexadecane was consumed during polymerization and the hydrocarbon-fluorocarbon interfacial tension increased after the polymerization as indicated by the reduction of interfacial area between hydrocarbon and fluorocarbon. A reluctance of the droplets to increase hydrocarbon-fluorocarbon interfacial area, which accompanied the Janus to double emulsion transition, can provide increased relative stability of the Janus droplet. In order to decouple the relative contributions from two factors, we designed the following experiment: Janus droplets after interfacial polymerization at 70% hydrocarbon-water surfactant were first tuned to H/F/W double emulsion at 35% hydrocarbon-water surfactant so that the polymer shells dissociated from the droplets and no longer affected the droplet morphology. These H/F/W double emulsions were then tuned back to various hydrocarbon-water surfactant volume ratios above 35% before checking their morphologies. The comparison of morphologies between "with shell," "after shell dissociation," and "without shell" is summarized in **Figure 6**.

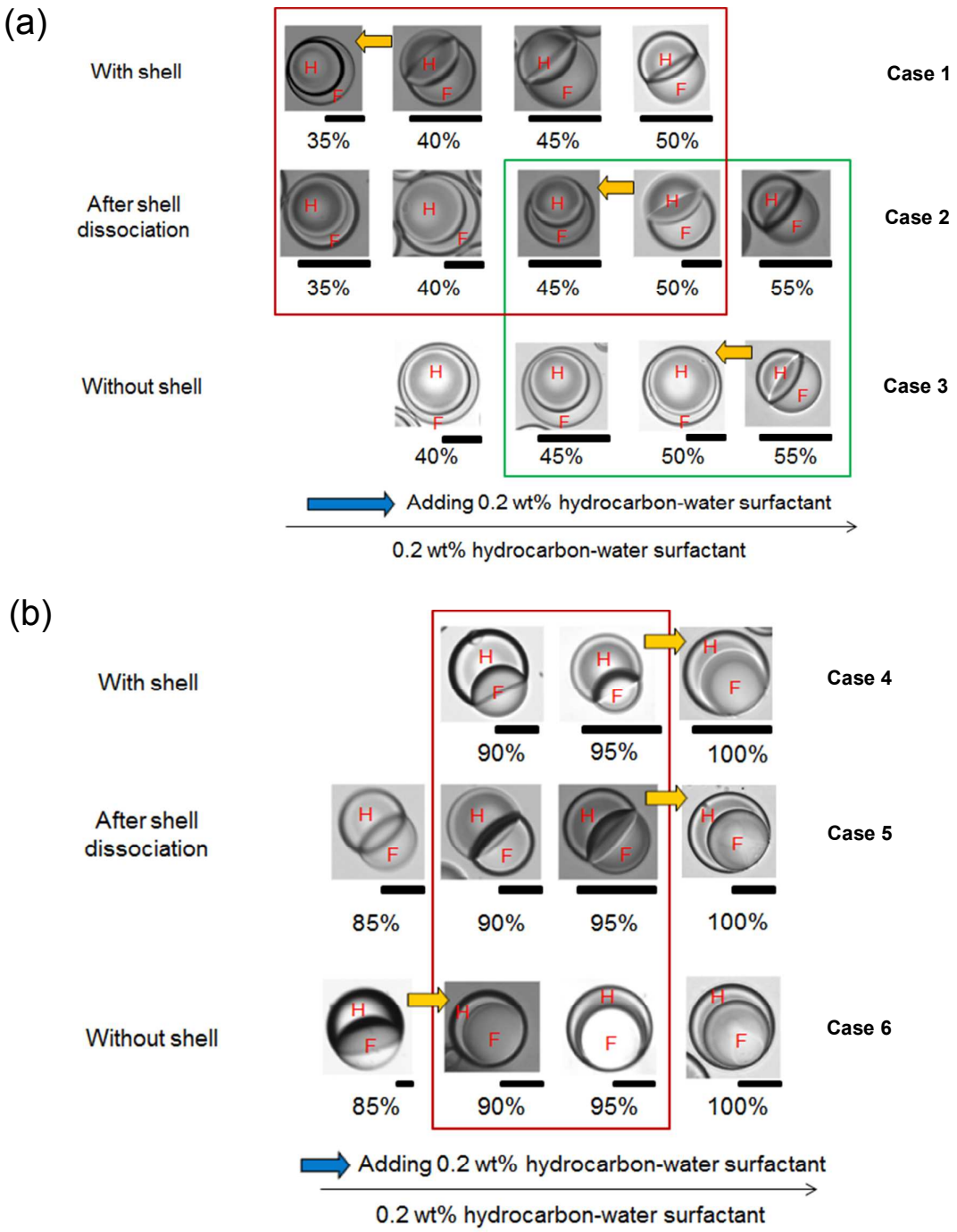

Figure 6. (a) Comparison of morphologies between "with shell (Case 1)", "after shell dissociation (Case 2)" and "without shell (Case 3)" going towards H/F/W (b) Morphology comparison between "with shell (Case 4)", "after shell dissociation (Case 5)" and "without shell (Case 6)" going towards F/H/W. The yellow arrow indicates a Janus to H/F/W transition, or a Janus to F/H/W transition; Scale bars: 50 μm

In **Figure 6a**, by comparing Case 2 and Case 3 where the only difference was monomer consumption in hexadecane, the Janus to H/F/W morphology transition occurred between 55% and 50% hydrocarbon-water surfactant when dibutyl maleate was not consumed (Case 3). However the same transition took place from 50% to 45% hydrocarbon-water surfactant when dibutyl maleate was consumed (Case 2). This result indicated that the range of Janus was extended 5% as a result of dibutyl maleate consumption in hexadecane. Similarly, by comparing the Case 1 and Case 2 wherein the only difference was the polymer shells, the Janus to H/F/W transition happened from 40% to 35% hydrocarbon-water surfactant with the polymer shells whereas the same transition took place from 50% to 45% hydrocarbon-water surfactant without the polymer shells. Hence, the polymer shells stabilized the Janus morphology over a range resulting from an increase of 10% of 0.2 wt% Zonyl solution. These results confirmed that polymer shell was the major reason for the Janus range expansion towards H/F/W. Indeed the polymer shells were amphiphilic and behaved as a highly effective and stable surfactant expanding the range of Janus towards H/F/W.

In **Figure 6b**, by comparing Case 4 and Case 5, the Janus to F/H/W transitions both occurred from 95% to 100% hydrocarbon-water surfactant regardless of whether the polymer shells were present. However, by comparing Case 5 and Case 6 where the only difference was the consumption of dibutyl maleate, Janus to F/H/W transition occurred from 85% to 90% hydrocarbon-water surfactant when dibutyl maleate was not consumed (Case 6) whereas the same transition happened from 95% to 100% hydrocarbon-water surfactant when dibutyl maleate was consumed (Case 5). These results showed that although polymer shell did not directly help stabilize the Janus morphology towards F/H/W, interfacial tension increase

associated with polymer shell formation contributed to the Janus range expansion towards F/H/W. This observation can be explained because our crosslinked polymer shell surfactants had a defined area and were pinned at the interface and thus cannot directly stabilize Janus morphology towards F/H/W. To further understand the effect hydrocarbon-fluorocarbon interfacial tension on droplet morphology, hexadecane with different wt% of dibutyl maleate and ethyl nonafluorobutylether were mixed and emulsified at various hydrocarbon-water surfactant volume ratios. We found that when hexadecane contained 12 wt% dibutyl maleate, the Janus to H/F/W transition occurred from 50% to 45% hydrocarbon-water surfactant, whereas the Janus to F/H/W transition occurred between 95% to 100% hydrocarbon-water surfactant (**Figure S4**). These transitions were close to the case wherein our polymer shells dissociated from the droplets. This observation verified that the Janus range expansion towards F/H/W was related to a decrease in wt% of dibutyl maleate in hexadecane as a result of its incorporation into the polymer shell.

Conclusions

In summary, we have developed stabilized Janus morphologies in dynamic complex liquid emulsion without harming their optical transparency in z-direction. The selective formation of polymer surfactant shells on the hydrocarbon hemisphere of the Janus droplets endowed them with extra stability. They displayed resistance to morphology changes upon external chemical perturbation and the range of Janus morphology was nearly doubled compared to the Janus droplets without hemispherical shells. This phenomenon can be explained by the surfactant nature of the polymer shell itself as well as the interfacial tension increase between hydrocarbon and fluorocarbon due to polymer shell formation. We foresee

great potential of using these stabilized Janus droplets as chemical/biological sensing platform as well as components for dynamic microlens arrays.

Supporting information

Supporting information is available free of charge on the ACS Publication website at DOI:

Interfacial polymerization experiments; Interfacial tension between hydrocarbon and fluorocarbon vs. dibutyl maleate wt%; θ_F vs. hydrocarbon-water surfactant volume ratio; Light transmission experiments; Janus to H/F/W and Janus to F/H/W transition at 12 wt% dibutyl maleate; Extended regular phase diagrams and modified phase diagrams; Examples of uniform droplet morphology in a full image; ^{1}H and ^{13}C NMR of **6**, **7** and **3**; Videos of a fluorescent hemispherical shell and the bottom portion of a fluorescent hemispherical shell

Acknowledgement

This work was supported by the National Science Foundation (NSF) Center for Energy Efficient Electronics Science (E3S) (Award ECCS-0939514) and the Army Research Office through the Institute for Soldier Nanotechnologies. We thank Mr. Jeffrey Wyckoff for assistance with confocal laser scanning microscope.

Reference

(1) Shao, D.; Li, J.; Zheng, X.; Pan, Y.; Wang, Z.; Zhang, M.; Chen, Q. X.; Dong, W. F.; Chen, L. Janus "nano-Bullets" for Magnetic Targeting Liver Cancer Chemotherapy. *Biomaterials* **2016**, *100*, 118–133.

(2) Aliño, V. J.; Pang, J.; Yang, K. L. Liquid Crystal Droplets as a Hosting and Sensing Platform for Developing Immunoassays. *Langmuir* **2011**, *27*, 11784–11789.

(3) Lone, S.; Cheong, I. W. Fabrication of Polymeric Janus Particles by Droplet Microfluidics. *RSC Adv.* **2014**, *4*, 13322.

(4) Kim, J. W.; Utada, A. S.; Fernández-Nieves, A.; Hu, Z.; Weitz, D. A. Fabrication of Monodisperse Gel Shells and Functional Microgels in Microfluidic Devices. *Angew. Chemie - Int. Ed.* **2007**, *46*, 1819–1822.

(5) Shum, H. C.; Abate, A. R.; Lee, D.; Studart, A. R.; Wang, B.; Chen, C. H.; Thiele, J.; Shah, R. K.; Krummel, A.; Weitz, D. A. Droplet Microfluidics for Fabrication of Non-Spherical Particles. *Macromol. Rapid Commun.* **2010**, *31*, 108–118.

(6) Lawrence, M. J.; Rees, G. D. Microemulsion-Based Media as Novel Drug Delivery Systems. *Adv. Drug Deliv. Rev.* **2000**, *45*, 89–121.

(7) Zhao, C.; Danish, E.; Cameron, N. R.; Kataky, R. Emulsion-Templated Porous Materials (PolyHIPEs) for Selective Ion and Molecular Recognition and Transport : Applications in Electrochemical Sensing. *J. Mater. Chem.* **2007**, *17*, 2446.

(8) Augustin, M. A.; Hemar, Y. Nano- and Micro-Structured Assemblies for Encapsulation of Food Ingredients. *Chem. Soc. Rev.* **2009**, *38*, 902–912.

(9) McClements, D. J.; Li, Y. Structured Emulsion-Based Delivery Systems: Controlling the Digestion and Release of Lipophilic Food Components. *Adv. Colloid Interface Sci.* **2010**, *159*, 213–228.

(10) Takei, H.; Shimizu, N. Gradient Sensitive Microscopic Probes Prepared by Gold Evaporation and Chemisorption on Latex Spheres. *Langmuir* **1997**, *13*, 1865–1868.

(11) Han, Y. D.; Kim, H.-S.; Park, Y. M.; Chun, H. J.; Kim, J.-H.; Yoon, H. C. Retroreflective Janus Microparticle as a Nonspectroscopic Optical Immunosensing Probe. *ACS Appl. Mater. Interfaces* **2016**, *8*, 10767–10774.

(12) Nisisako, T.; Torii, T.; Takahashi, T.; Takizawa, Y. Synthesis of Monodisperse Bicolored Janus Particles with Electrical Anisotropy Using a Microfluidic Co-Flow System. *Adv. Mater.* **2006**, *18*, 1152–1156.

(13) Kim, S. H.; Jeon, S. J.; Jeong, W. C.; Park, H. S.; Yang, S. M. Optofluidic Synthesis of Electroresponsive Photonic Janus Balls with Isotropic Structural Colors. *Adv. Mater.* **2008**, *20*, 4129–4134.

(14) Wu, Y.; Lin, X.; Wu, Z.; Möhwald, H.; He, Q. Self-Propelled Polymer Multilayer Janus Capsules for Effective Drug Delivery and Light-Triggered Release. *ACS Appl. Mater. Interfaces* **2014**, *6*, 10476–10481.

(15) Walther, A.; Müller, A. H. E. Janus Particles: Synthesis, Self-Assembly, Physical Properties, and Applications. *Chem. Rev.* **2013**, *113*, 5194–5261.

(16) Yang, S.; Guo, F.; Kiraly, B.; Mao, X.; Lu, M.; Leong, K. W.; Huang, T. J. Microfluidic Synthesis of Multifunctional Janus Particles for Biomedical Applications. *Lab Chip* **2012**, *12*, 2097.

(17) Nisisako, T.; Tonii, T. Formation of Biphasic Janus Droplets in a Microfabricated

Channel for the Synthesis of Shape-Controlled Polymer Microparticles. *Adv. Mater.* **2007**, *19*, 1489–1493.

(18) Roh, K.-H.; Martin, D. C.; Lahann, J. Biphasic Janus Particles with Nanoscale Anisotropy. *Nat. Mater.* **2005**, *4*, 759–763.

(19) Nisisako, T.; Torii, T.; Higuchi, T. Novel Microreactors for Functional Polymer Beads. *Chem. Eng. J.* **2004**, *101*, 23–29.

(20) Nie, Z.; Li, W.; Seo, M.; Xu, S.; Kumacheva, E. Janus and Ternary Particles Generated by Microfluidic Synthesis: Design, Synthesis, and Self-Assembly. *J. Am. Chem. Soc.* **2006**, *128*, 9408–9412.

(21) Bucaro, M. A.; Kolodner, P. R.; Ashley Taylor, J.; Sidorenko, A.; Aizenberg, J.; Krupenkin, T. N. Tunable Liquid Optics: Electrowetting-Controlled Liquid Mirrors Based on Self-Assembled Janus Tiles. *Langmuir* **2009**, *25*, 3876–3879.

(22) Zarzar, L. D.; Sresht, V.; Sletten, E. M.; Kalow, J. A.; Blankschtein, D.; Swager, T. M. Dynamically Reconfigurable Complex Emulsions via Tunable Interfacial Tensions. *Nature* **2015**, *518*, 520–524.

(23) Kaewsaneha, C.; Tangboriboonrat, P.; Polpanich, D.; Eissa, M.; Elaissari, A. Janus Colloidal Particles: Preparation, Properties, and Biomedical Applications. *ACS Appl. Mater. Interfaces.* **2013**, *5*, 1857–1869.

(24) Hann, S. D.; Niepa, T. H. R.; Stebe, K. J.; Lee, D. One-Step Generation of Cell-Encapsulating Compartments via Polyelectrolyte Complexation in an Aqueous Two Phase System. *ACS Appl. Mater. Interfaces.* **2016**, *8*, 25603–25611.

(25) Scott, C.; Wu, D.; Ho, C.-C.; Co, C. C. Liquid-Core Capsules via Interfacial Polymerization: A Free-Radical Analogy of the Nylon Rope Trick. *J. Am. Chem. Soc.* **2005**, 4160–4161.

(26) Bell, T. D. M.; Yap, S.; Jani, C. H.; Bhosale, S. V.; Hofkens, J.; Schryver, F. C. De; Langford, S. J.; Ghiggino, K. P. Synthesis and Photophysics of Core-Substituted Naphthalene Diimides: Fluorophores for Single Molecule Applications. *Chem. - An Asian J.* **2009**, *4*, 1542–1550.

(27) Zhang, L.; Cai, L.-H.; Lienemann, P. S.; Rossow, T.; Polenz, I.; Vallmajo-Martin, Q.; Ehrbar, M.; Na, H.; Mooney, D. J.; Weitz, D. A. One-Step Microfluidic Fabrication of Polyelectrolyte Microcapsules in Aqueous Conditions for Protein Release. *Angew. Chemie Int. Ed.* **2016**, 13470–13474.

(28) Maleki, M.; Fried, E. Multidomain and Ground State Configurations of Two-Phase Vesicles. *J. R. Soc. Interface* **2013**, *10*, 20130112.

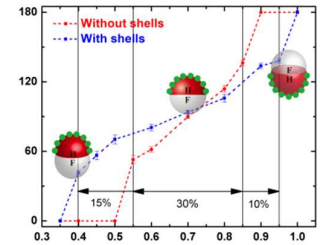

Polymeric Hemispherical Shells Increased Janus Droplet Stability